



Contents lists available at ScienceDirect

Nuclear Instruments and Methods in Physics Research A

journal homepage: www.elsevier.com/locate/nima

Air fluorescence relevant for cosmic-ray detection—Review of pioneering measurements

Fernando Arqueros^a, Jörg R. Hörandel^b, Bianca Keilhauer^{c,*}

^a Facultad de Ciencias Físicas, Universidad Complutense de Madrid, E-28040 Madrid, Spain

^b Department of Astrophysics, Radboud Universiteit Nijmegen, P.O. Box 9010, 6500 GL Nijmegen, The Netherlands

^c Institut für Experimentelle Kernphysik, Universität Karlsruhe, Postfach 3640, 76021 Karlsruhe, Germany

ARTICLE INFO

Available online 19 August 2008

Keywords:

Fluorescence yield
Air showers

ABSTRACT

Cosmic rays with energies exceeding 10^{17} eV are frequently registered by measurements of the fluorescence light emitted by extensive air showers. The main uncertainty for the absolute energy scale of the measured air showers is coming from the fluorescence light yield of electrons in air. The fluorescence light yield has been studied in laboratory experiments. Pioneering measurements between 1954 and 2000 are reviewed.

© 2008 Elsevier B.V. All rights reserved.

1. Introduction

Cosmic rays with energies exceeding 10^{17} eV are frequently observed by measurements of the fluorescence light emitted in air showers. The latter are induced by high energy cosmic rays interacting in the Earth's atmosphere initiating a cascade of secondary particles. Relativistic electrons (and positrons) are the most numerous charged particles in air showers. On their way through the atmosphere they excite nitrogen molecules. The nitrogen molecules release their excitation energy partly through isotropic emission of fluorescence light. The fluorescence light is measured with imaging telescopes in air shower experiments, allowing for a three-dimensional reconstruction of the shower profile in the atmosphere. The main uncertainty of the absolute energy scale of the measured showers is coming from the fluorescence light yield of electrons in air.

The bulk of the fluorescence light is induced by electrons with MeV energies. Thus, the emission mechanism can be studied in laboratory experiments using particles, mainly electrons, from radioactive sources or particle accelerators. Particles are injected into volumes of nitrogen and air under well controlled circumstances and the fluorescence light yield is measured as a function of various parameters, like electron energy, gas pressure, temperature, and humidity.

Recent developments have been discussed during the 5th Fluorescence Workshop in El Escorial, Spain, from September 16th to 20th, 2007. The results are summarized in an accompanying article [1]. The present article summarizes measurements of the

fluorescence light yield conducted between 1954 and 2000. The objective is to compile information relevant for air shower observations from the (sometimes hardly accessible) historical papers. Their implications on the contemporary understanding of the subject are discussed in Ref. [1].

2. A.E. Grün, E. Schopper (1954)

Very early investigations of fluorescence emission in gases induced by rapid particles were performed by Grün and Schopper [2]. In the experimental setup, described in the paper, α -particles from a radioactive Po-source were used to excite the gas. The measurements were done mainly in nitrogen gas and nitrogen argon mixtures, but also in nitrogen gas with different admixtures like Xe, O₂, etc. The fluorescence yield Φ^1 was defined as

$$\Phi(N, T, c, v) = \frac{\phi}{\varepsilon} \quad (1)$$

where ϕ is the radiation power in W/cm³ and ε is the deceleration power, also in W/cm³, of the primary particle stream in the gas. The fluorescence yield depends on N , the particle number density of the gas, T is the temperature of the gas, c is the concentration of the admixture to the nitrogen, and v is the velocity of the exciting particles as it enters the gaseous volume. The radiation power was measured photo-electrically with a photomultiplier 1 P 28. The experimental setup was chosen carefully, since the measured stream of photons yields only the

* Corresponding author. Tel.: +34 913944681; fax: +34 913945193.
E-mail address: bianca.keilhauer@ik.fzk.de (B. Keilhauer).

¹ In the nomenclature of the summary article [1], the $\Phi(N, T, c, v)$ from Grün and Schopper corresponds to Φ_2 .

fluorescence yield under the following conditions, as stressed in the publication [2]:

- (1) The gas volume has to be independent of the variable which is varied during the measurement. Then the proportionality between the measured photo-stream and the radiation power ϕ is fulfilled.
- (2) The dependence of the decelerations power ε on the varied variable has to be known. The derived ratio ϕ/ε is proportional to the outer fluorescence yield.
- (3) The emitted radiation must not be absorbed by the gas itself. This ensures that the outer yield is equal the inner fluorescence yield.
- (4) The spectral combination of the radiation must be constant because of the selective sensitivity of the photo-cathode.

Additionally, the setup was such that no α -particle hits any wall within the measurement volume. To account for deceleration of the exciting particles before and in the observed volume under high-pressure conditions, a pressure-dependent correction factor was introduced.

Firstly, the pressure-dependence of the fluorescence yield $\Phi(p)$ was measured for constant temperature T . The fluorescence yield was written in dependence on pressure p^2 as

$$\Phi(p) = \frac{\Phi_0}{1 + p/p'} \quad \text{with } p' = \frac{p_0 \gamma_0}{\delta(T) N_0} = p_0 \frac{\tau_L}{\tau_0} \quad (2)$$

with $\tau_L = 1/\delta N_0$ as the mean lifetime of the excited molecule with respect to quenching. Φ_0 is the yield for $N \rightarrow 0$ meaning maximal yield. γ_0 is defined as $1/\tau_0$, where τ_0 is the mean lifetime without quenching. δ means the “quenching velocity” and can be given as

$$\delta = \delta(T) = u(T) \cdot \sigma_L(T). \quad (3)$$

$u(T)$ is the mean relative velocity of the gas molecules and $\sigma_L(T)$ is the temperature-dependent quenching cross-section. In pure nitrogen, the fit to the data points led to a value of $p'_{N_2} = 35$ Torr [2]. The authors concluded a ratio between τ_L and τ_0 of 0.05 at 760 Torr and 20 °C. The estimated mean lifetime τ_L of the $C^3\Pi_u$ -state of N_2 -molecules with respect to quenching was about 5×10^{-10} s with $\tau_0 \approx 10^{-8}$ s. It was pointed out that the quenching cross-section σ_L is smaller by a factor of $\frac{1}{2.5}$ compared with the gas-kinetic cross-section of N_2 -molecules.

Secondly, the temperature dependence of the fluorescence yield was discussed. It was stated that this dependence is caused by the temperature dependence of the quenching process. Measured data were plotted for the function $\delta(T)$. The authors concluded that the quenching cross-section σ_L decreases with increasing temperature apart from a \sqrt{T} -increase of the mean relative velocity u of molecules with increasing temperature.

Thirdly, the role of secondary electrons and the concentration-dependent light yield of Ar- N_2 -mixtures was analyzed [2]. The spectroscopic investigation started with pure argon and N_2 was added successively. In pure Ar, the radiation power stems from Ar spark lines induced by ionization. In pure nitrogen, the emission comes mainly from the second positive system and smaller contributions from N_2^+ . It was found that already at small concentrations of N_2 , the light yield is significantly increased. The authors explained it by an energy transfer from Ar to N_2 . The deceleration power of the incoming particles is absorbed by both gases and part of the energy absorbed by argon is transferred to nitrogen which then radiates fluorescence light. The idea of

energy transfer is supported by the fact that the $C^3\Pi_u$ -state of N_2 cannot be excited directly by primary particles. The obtained concentration-dependent light yield curve is the result of the concentration dependence of the energy transfer and of concentration-dependent quenching. The steep increase of the yield curve already at small nitrogen concentrations was explained by the authors with large cross-sections for the process of energy transfer. With increasing nitrogen concentration, the energy transfer saturates and decreases afterwards because of the decreasing Ar-concentration. Additionally, the quenching due to argon in the nitrogen gas superimposes. In conclusion, it was stated that the energy transfer occurs mainly due to secondary electrons from argon.

3. A.E. Grün (1958)

Three years later, Grün published measurements of fluorescence yield in air [3]. He used a parallel, narrow beam of electrons with energies between 4.2 and 43.7 keV. The aim of the investigation was to determine the light yield as a function of the gas density. Therefore, the function $\Phi(p)$ was measured at constant temperature $T = 20$ °C within the pressure range from 10 to 600 mm Hg. From a description of the fluorescence mechanism, Grün deduced the proportionality³

$$1/\Phi \propto 1 + p/p'. \quad (4)$$

A linear fit to the data points yielded a $p' = 11.5$ mm Hg for air as an average over a large spectral range.

In the following years, the aurora phenomena in the Earth's atmosphere came more and more into focus. Several investigations about light yield, excitation and de-excitation processes were carried out. These studies were performed in pure nitrogen or air, because also the aurora phenomena are mainly nitrogen scintillation high up in the atmosphere. Here, only some of the experiments are mentioned exemplarily whose results are used later in the discussions about nitrogen fluorescence induced by extensive air showers.

4. B. Brocklehurst (1964)

In 1964, Brocklehurst published quenching parameters for nitrogen–nitrogen and nitrogen–oxygen collisional de-excitation [4]. To this end, he measured the light emission in pure nitrogen gas and in nitrogen–oxygen mixtures within a pressure range of 1–750 mm Hg. The excitation was performed by soft X-rays. The spectrum was presumably continuous between 5 and 45 keV with a maximum intensity at about 25–30 keV. The emission spectra were observed using a spectrograph and intensity measurements were done with a 1 P 28 photomultiplier. Main contributions to the light yield were identified to be of the second positive bands ($C^3\Pi_u \rightarrow B^3\Pi_g$) of N_2 and of the first negative bands ($B^2\Sigma_u^+ \rightarrow X^2\Sigma_g^+$) of N_2^+ .

For studying the kinetics of collisional processes, the pressure was chosen to be higher than 1 mm Hg, since above this value the excitation conditions are independent of pressure [4]. It is mentioned that secondary electrons cause excitation above 10^{-2} mm Hg, but are completely absorbed in the gas for pressure higher than 1 mm Hg. Furthermore, the excitation is assumed to be without ion recombination processes. Former measurements are cited in the publication by Brocklehurst [4] showing that fields applied for the removal of ions do not have any effect on the light output. An iterative procedure was applied in the analysis of the

² In the nomenclature of the summary article [1], the p from Grün and Schopper corresponds to P and p' to P_v .

³ For the nomenclature of the summary article [1], see footnotes of Section 2.

Table 1
Quenching parameters given in Brocklehurst [4]

Upper state	ν'	Quencher	k (mm ⁻¹)	σ (Å ²)
C ³ Π _u	0	N ₂	0.015 ± 0.002	0.38 ± 0.09
	1		0.041 ± 0.004	1.04 ± 0.22
	2		0.047 ± 0.010	1.2 ± 0.35
B ² Σ _u ⁺	0, 1	O ₂	0.45 ± 0.15	12 ± 5
	0	N ₂	0.85 ± 0.3	15 ± 5
	0	O ₂	0.8 ± 0.4	14 ± 7

quenching parameters for separating between 1N and 2P states of nitrogen. The factor k , which is given in the publication, corresponds to P in modern nomenclature. The necessary fits to the data were done in the low-pressure range up to 150 mm Hg for 2P and up to 40 mm Hg for 1N. For higher pressure, quenching effects make the data points deviate from the linear dependence found at low pressure. To extract collisional cross-sections, the author used the lifetimes from Bennett and Dalby [5] which are $(4.45 \pm 0.6) \times 10^{-8}$ s for the 2P system and $(6.58 \pm 0.35) \times 10^{-8}$ s for the 1N system. The results are listed in Table 1.

5. G. Davidson, R. O'Neil (1964)

For determining the characteristics of the spectra radiated from certain gases, Davidson and O'Neil bombarded nitrogen and air with 50 keV electrons [6]. The main results have been the efficiencies for the conversion of electron energy to optical radiation for about 100 transitions in air and nitrogen between 320 and 1080 nm. The pressure for this investigation was fixed at 600 Torr. The radiation was spectrally analyzed by a monochromator with either a RCA 6199 photomultiplier with S-11 response or a liquid nitrogen cooled RCA 7102 photomultiplier with S-1 response. The system was calibrated absolutely using a standard tungsten ribbon filament lamp and a 1000 °C blackbody radiation. The absolute fluorescent efficiency for a given spectral component was defined as the ratio of power radiated by the spectral feature to the incident electron beam power. The estimated error for the efficiency was determined to be ±15% due to the absolute radiance calibration and the beam current measurement. The authors listed the integrated intensities of the observed spectra in terms of absolute fluorescent efficiencies in a table [6]. The given wavelengths are band-head wavelengths after Wallace [7]. Since the data of the publication [6] were updated in the full report about the work of Davidson and O'Neil [8], here no data are reviewed and the reader is referred to Section 7.

6. A.N. Bunner (1967)

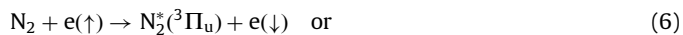
The first study of nitrogen fluorescence emission with respect to cosmic-ray detection was performed by Bunner in the mid-1960s, when Bunner published his thesis [9] and PhD thesis [10]. Bunner accurately discussed excitation and de-excitation processes. It is stressed that for pressure down to values corresponding to atmospheric altitudes of about 60 km a.s.l., the fluorescence spectrum consists almost entirely of the second positive N₂ system (2P) and the first negative N₂⁺ system (1N).

The upper level of 1N can be excited directly



However, the upper levels of the 2P system cannot be excited directly by high energy interactions because of forbidden changes in the electronic spin. At lower velocities of the incoming electrons, the resultant spin change is possible, which is tantamount to excitation

by low energetic secondary electrons. Also cascading from higher levels may excite the 2P system:



In the absence of collisional quenching, the absolute intensity of a band is proportional to $N_{\nu'} A_{\nu'\nu''}$, where $N_{\nu'}$ is the number of molecules per unit volume in the state ν' , and $A_{\nu'\nu''}$ is the transition probability for a radiative transition from the level ν' to the level ν'' , so-called Einstein coefficients. For an approximate calculation of the distribution of populations in various excited states, the Frank–Condon principle was used, which means that molecular electronic transitions occur so rapidly that the internuclear separation stays constant. Bunner summarized several excitation channels by the following equation:

$$\frac{2P \text{ excitations}}{\text{cm}} = N \sigma_{2P}^e(E) + N \int_0^{E_{\max}} \sigma_{\text{ion}}^e(E, E') S(E') dE' + N \sigma_A^e(E) S(E_A). \quad (8)$$

The first term describes the number of excitations of level ν per cm³ and second, where N is the number of molecules per cm³ and σ_{2P}^e gives the cross-section for excitation of a level ν by electron incident with energy E . The second term describes the number of excitation from secondary electrons produced by ionization. The ionization potential of N₂ is 15.7 eV, whereas the average energy loss per ion pair in air is about 34 eV. Thus, the ionization results in a distribution of secondary electrons, so-called delta rays, having typically several eV energy, sufficient to excite both the B²Σ_u⁺ level and the C³Π_u level of N₂ [10]. The third term accounts for the excitations from Auger electrons. Since a high energy electron has about equal probability of interacting with any atomic electron, a certain number of ionizations will liberate K-electrons and lead to the emission of Auger electrons, which on their part can excite nitrogen.

The de-excitation process was subdivided by Bunner into three parts: radiative transition to any lower state, collisional quenching, and internal quenching with the corresponding lifetimes τ_v , τ_c , and τ_i . In further considerations, Bunner did not differentiate between the first and last de-excitation channel anymore and introduced the nomenclature of⁴

$$\frac{1}{\tau_0} = \frac{1}{\tau_v} + \frac{1}{\tau_i}. \quad (9)$$

The fluorescence efficiency is then defined as $(\tau_0/\tau_v)/(1 + \tau_0/\tau_c)$ photons per excitation. The lifetime due to collisional quenching can be described by kinetic gas theory: $\tau_c = 1/(\sqrt{2}N\sigma_{\text{nn}}\bar{v})$, where σ_{nn} is the cross-section for nitrogen–nitrogen quenching and \bar{v} the mean molecular velocity = $\sqrt{(8kT)/(\pi M)}$, with k is the Boltzmann constant, T the temperature of the gas, and M the molecular mass. After several conversions and introducing p' as a reference pressure, the fluorescence efficiency is then written as⁵

$$\text{fluorescent efficiency} = \frac{(\tau_0/\tau_v)}{1 + p/p'} \quad (10)$$

Thus, τ_0 is the fluorescence decay time in the absence of collisional quenching. For the fluorescence emission in air, Bunner expanded the given definition by a term accounting for nitrogen–oxygen quenching [10]:

$$\frac{1}{\tau_{\text{no}}} = 2N_o\sigma_{\text{no}}\sqrt{\frac{2kT(M_n + M_o)}{\pi M_n M_o}} \quad (11)$$

⁴ In the nomenclature of the summary article [1], the τ_0 from Bunner corresponds to τ_v^+ .

⁵ Compare with (23) of Ref. [1].

Table 2
Deactivation constants for nitrogen and air given in Bunner [10]

	$p'(N_2)$ (mmHg)	$p'(\text{air})$ (mmHg)	σ_{no} (cm ²)	σ_{nn} (cm ²)	$\tau_0 \times 10^8$ (s)
1N					
$v=0$	1.49	1.08	13×10^{-15}	4.37×10^{-15}	6.58 ± 0.35
2P					
$v=0$	90	15	2.1×10^{-15}	1.0×10^{-16}	4.45 ± 0.6
$v=1$	24.5	6.5		3.5×10^{-16}	4.93
$v=2$	10.9	4.6		8.8×10^{-16}	4.45
$v=3$	5.4	2.5		1.2×10^{-15}	6.65

which yields a

$$\text{fluorescent efficiency} = \frac{(\tau_0/\tau_v)}{1 + \tau_0 \left(\frac{1}{\tau_{nn}} + \frac{1}{\tau_{no}} \right)} \quad (12)$$

with σ_{no} as the effective nitrogen–oxygen collisional cross-section for de-excitation, N_0 is the number of oxygen molecules per cm³, and M_n and M_o are the nitrogen and oxygen molecular masses.

In Ref. [10], Bunner compared several measurements and stressed that the upper equations are only valid under thin target conditions.⁶ For high-pressure conditions, he compared his own measurements performed during the studies for his thesis with those from Davidson and O'Neil [6] and concludes a fair agreement. As a basis of further calculations, he summarized deactivation constants for nitrogen and air at a gas temperature of about 300 K, see Table 2.

Bunner discussed several experiments, e.g. Grün and Schopper [2], Davidson and O'Neil [6], Brocklehurst [4] as reviewed in this article in large detail.

In the following, some discussions about quenching and dependences on gaseous conditions are reviewed. Bunner stressed that the quenching mechanism is not well understood. The cross-sections for collisional quenching seem to be larger than their molecular radii as given by gas-kinetic theory. Furthermore, the cross-sections appear to be generally higher for higher vibrational excitation, except for the 1N system of nitrogen. It was pointed out that molecular oxygen is a very efficient quencher due to its permanent dipole moment and the many low-lying energy levels to which excitation energy may be transferred in a collision [10]. Also some recombination reactions were discussed, but none of them has important effects on nitrogen fluorescence in the atmosphere. The 1% argon content of air might yield additional fluorescence emission because of a high cross-section for argon excitation by electrons. However, experiments on argon–nitrogen mixtures have verified de-excitations of argon due to quenching processes. Bunner concluded an expectation of less than 1% for the argon contribution to the 2P nitrogen emission in air. The fluorescence yield depends also on temperature and pressure. Thus, a day-to-day or seasonal variation and a altitude-dependent variation has to be considered. The deactivation cross-sections are taken to be independent of temperature. The day-to-day variations vary the fluorescence efficiency in the order of 1%, assuming a mean temperature of 290 K and a 5% temperature change. Difference of about 20 K, as between summer and winter, leads to a reduction of the fluorescence yield up to 4% for the lower temperature. With increasing altitude, the temperature decreases and at about 10 km a.s.l. it is lower by 60 K which reduces the efficiency by 11%.

⁶ For a definition of thin target vs. thick target conditions, read the accompanying summary article [1].

Table 3
Predictions for cosmic-ray fluorescence in the lower atmosphere given in Bunner [10]

Band	λ (Å)	$E(\lambda_i)$ (%)	p' (mm)	Sea level efficiency	
				$\times 10^{-4}\%$	Photons/MeV
1N					
0-0	3914	0.33	1.0	4.33	1.37
2P					
0-0	3371	0.0820	15	15.9	4.32
0-1	3577	0.0615		11.9	3.44
0-2	3805	0.0213		4.12	1.27
0-3	4059	0.0067		1.30	0.48
1-0	3159	0.050	6.5	4.3	1.09
1-1	3339	0.0041		0.35	0.094
1-2	3537	0.0290		2.48	0.71
1-3	3756	0.0271		2.31	0.73
1-4	3998	0.0160		1.36	0.44
2-1	3136	0.029	4.6	0.96	0.23
2-2	3309	0.0020		0.12	0.032
2-3	3500	0.0040		0.24	0.068
2-4	3711	0.0100		0.60	0.18
2-5	3943	0.0064		0.38	0.12
3-2	3117	0.005	2.5	0.16	0.04
3-3	3285	0.0154		0.50	0.13
3-4	3469	0.0063		0.21	0.06
3-5	3672	0.0046		0.15	0.045
3-6	3894	0.003		0.10	0.03
3-7	4141	0.0017		0.056	0.02

Here, only the contributions between 300 and 420 nm are reviewed.

Finally, Bunner calculated the fluorescence emission in the lower atmosphere as a prediction for cosmic-ray-induced scintillation. The set of best self-consistent quenching parameters used is reviewed in Table 2. Additionally, Bunner applied absolute fluorescent efficiencies in absence of quenching from Hartman [11], Bunner [9], and Davidson and O'Neil [6]. The agreement between these measurements is fair. For the calculation, Bunner used a set of weighted averages for the fluorescence efficiency for high energy electrons [10]. In Table 3,⁷ Bunner's calculations for the fluorescence emission are given which were used by all cosmic-ray experiments as the standard reference for many decades.

7. R. O'Neil, G. Davidson (1968)

The former publication of these two authors was embedded in a multi-year project (1964–1967) for the *Air Force Cambridge Research Laboratories, Office of Aerospace Research, United States Air Force, Bedford, Massachusetts*. The aim of this project was the interpretation of the nature of the optical emissions for atmospheric constituents excited by energetic electrons in a controlled laboratory experiment for understanding ionospheric radiative phenomena, including natural aurora and airglow emissions as well as the optical emissions associated with the detonation of a nuclear device. In the final report [8], revised values of the absolute fluorescent efficiencies published in Ref. [6] were presented. Essentially, the earlier values were confirmed to the order of 10–20%. The entire project covers measurements for thick and thin target in nitrogen and air.

For the thick target case (see footnote 6), fluorescent efficiencies were obtained at a pressure of 22 Torr excited by

⁷ In the nomenclature of the summary article [1], $E(\lambda_i)$ from Bunner corresponds to Φ_{λ}^0 , the sea level efficiency in % to Φ_{λ} , and the sea level efficiency in Photons/MeV to Y_{λ} .

Table 4
Spectral fluorescent efficiencies ε of nitrogen and air at 600 Torr given in O'Neil and Davidson [8]

λ (Å)	Molecule or atom	Band or line(s)	N ₂ fl. eff.		Air fl. eff.	
			($\times 10^{-7}$)	Rem. ^a	($\times 10^{-7}$)	Rem. ^a
3285	N ₂	2P(3–3)	44	SO	6.4	I
3371	N ₂	2P(0–0)	4300	I	210	I
3469	N ₂	2P(3–4)	11	PO	2.6	SO
3501	N ₂	2P(2–3)	2.0	PO
3537	N ₂	2P(1–2)	440	SO	30	SO
3577	N ₂	2P(0–1)	3000	I	140	I
3672	N ₂	2P(3–5)	17	PO	1.9	SO
3711	N ₂	2P(2–4)	72	SO	7.7	I
3756	N ₂	2P(1–3)	340	I	31	I
3805	N ₂	2P(0–2)	1180	I	53	I
3853	CN ^b		200	SO
3914	N ₂ ⁺	1N(0–0)	120	I	70	I
3943	N ₂	2P(2–5)	80	PO	4.8	PO
3998	N ₂	2P(1–4)	180	I	18	I
4059	N ₂	2P(0–3)	360	I	18	I
4142	N ₂ , CN ^c		38	SO	1.3 ^d	SO
4201	CN, N ₂ ^e		90	SO	3.5 ^f	I

^a When more than one identification is given the fluorescent efficiency refers to the identified source as a single spectral feature. The symbols indicate the estimated accuracy of the relative fluorescent efficiencies as follows: I, isolated, $\pm 10\%$; SO, slightly overlapped, $\pm 20\%$; PO, partially overlapped, $\pm 35\%$. The error in the absolute measurement is estimated to be an additional $\pm 15\%$.

^b CN violet—main system, transitions (4–4), (3–3), (2–2), (1–1), (0–0).

^c N₂ and CN violet—main system, transitions 2P(3–7), CN (5–6), (4–5).

^d Only for the transition 2P(3–7); the CN transitions have not been observed in air.

^e CN violet—main system and N₂, transitions (3–4), (2–3), 2P(2–6).

^f Only for the transition 2P(2–6); the CN transitions have not been observed in air.

10 keV electrons and at 600 Torr excited by 50 keV electrons. The spectra were observed in the wavelength region between 2000 and 11000 Å, but the efficiencies were only presented above 3200 Å, because of impurities in the spectrum from NO γ bands between 2000 and 3200 Å. The band systems observed were the second positive ($C^3\Pi_u \rightarrow B^3\Pi_g$), first positive ($B^3\Pi_g \rightarrow A^3\Sigma_u^+$), Gaydon–Green and Herman infrared systems of N₂ and the first negative system ($B^2\Sigma_u^+ \rightarrow X^2\Sigma_g^+$) of N₂⁺. In addition, the NO γ system ($A^2\Sigma^+ \rightarrow X^2\Pi$), CN violet ($B^2\Sigma^+ \rightarrow X^2\Sigma^+$), and red systems ($A^2\Pi_i \rightarrow X^2\Sigma^+$) were observed as impurities in the target chamber. The revised spectral fluorescent efficiencies can be found in Table 4.⁸ Here, only the contributions between 320 and 420 nm are repeated.

The N₂⁺ first negative system was studied in more detail. The efficiencies were measured for many combinations of incident electron energy (10–60 keV) and nitrogen gas pressure (22–800 Torr). The resulting linear relationship indicates that the fluorescent efficiency is independent of electron energy and that the Stern–Volmer mechanism describes the quenching process of the 391.4 nm emission:

$$\frac{1}{\varepsilon} = \frac{1}{\varepsilon_0} (1 + 2.2 \times 10^{21} \cdot \sigma \tau P). \quad (13)$$

Here, ε is the fluorescent efficiency at any pressure, ε_0 ⁹ the fluorescent efficiency at low pressure where quenching can be neglected, σ the deactivation cross-section of the neutral nitrogen molecule in cm², τ the lifetime of the 391.4 nm band in seconds

⁸ In the nomenclature of the summary article [1], ε from Davidson and O'Neil corresponds to Φ_z .

⁹ In the nomenclature of the summary article [1], ε_0 from Davidson and O'Neil corresponds to Φ_z^0 .

Table 5
Collisional deactivation cross-sections of N₂ and air for the second positive bands of N₂ given in O'Neil and Davidson [8]

Transition	N ₂ ($\times 10^{-16}$) cm ²	Air ($\times 10^{-15}$) cm ²
(0–0)	0.56 \pm 0.08	0.95 \pm 0.15
(0–1)	0.50 \pm 0.08	0.85 \pm 0.13
(0–2)	0.51 \pm 0.07	1.0 \pm 0.16
(0–3)	0.49 \pm 0.07	1.0 \pm 0.16
(0–4)	0.50 \pm 0.08	1.0 \pm 0.16
(0–5)	0.85 \pm 0.20	
(1–2)	1.4 \pm 0.4	1.5 \pm 0.3
(1–3)	1.2 \pm 0.15	1.4 \pm 0.3
(1–4)	1.4 \pm 0.2	1.3 \pm 0.2
(1–6)	1.3 \pm 0.2	1.6 \pm 0.6
(1–7)		1.3 \pm 0.2
(2–4)	1.5 \pm 0.4	1.1 \pm 0.2
(2–6)		1.5 \pm 0.3
(2–7)		1.1 \pm 0.2

and P the pressure in Torr. From their thin target measurements, the authors obtained $\varepsilon_0 = (6.0 \pm 1.0) \times 10^{-3}$ in nitrogen for excitation by electrons with several hundred eV or more. Applying lifetime measurements from Bennett and Dalby [5] with $\tau = (6.58 \pm 0.35) \times 10^{-8}$ s, the N₂ collisional deactivation cross-section becomes $(5.9 \pm 1.4) \times 10^{-15}$ cm². Similar measurements were performed in air. The value of ε_0 in air was estimated to be 0.76 the value in N₂. Using the result for the cross-section in N₂, an O₂ quenching cross-section of $(1.4 \pm 1.0) \times 10^{-14}$ cm² was obtained. The emission at 391.4 nm was calibrated absolutely. The relative integrated intensities of the second positive system were converted into absolute fluorescent efficiencies by a conversion factor based on the known absolute value for the 391.4 nm band at a given target pressure. For further details see Ref. [8]. The collisional deactivation cross-sections of N₂ and air for the second positive bands can be found in Table 5. Analyzing several Stern–Volmer plots of the second positive bands in air and N₂, values for the fluorescent efficiencies ε_0 at pressures low enough to exclude quenching were derived by O'Neil and Davidson. The results for the first four band systems of the second positive system are repeated in Table 6. For the thin target case, the gas pressure was reduced so that the incoming electrons lost only a small fraction of their energy in crossing the observation region of the target chamber. A distinction between primary and secondary electron excitation was based on the spatial distribution of the emittance. However, detailed studies have been performed mainly for the Meinel bands of N₂⁺ [8].

8. Cross-section and lifetime data between 1969 and 2000

After these fundamental experiments on fluorescence emission for cosmic-ray experiments, Sections 2–7, several detailed studies on sets of cross-sections and radiative lifetimes have been published by many authors. Here only those of them are reviewed who are cited in the accompanying article [1] in discussions about fluorescence emission of extensive air showers.

8.1. Stanton and St. John (1969)

Stanton and St. John measured in 1969 the optical cross-sections for, amongst others, the first negative bands of N₂⁺ and introduced an apparent cross-section for excitations [12].

Table 6

Fluorescent efficiencies ε_0 for the N_2 second positive bands excited by energetic electron incident on N_2 and air given in O'Neil and Davidson [8]

Transition	$\varepsilon_0(\times 10^{-5})^a$		Ratio $\varepsilon_0(N_2)/\varepsilon_0(\text{Air})$
	N_2	Air	
0–0	186 ± 16	112 ± 15	1.7 ± 0.3
0–1	126 ± 10	82 ± 11	1.5 ± 0.2
0–2	48 ± 4	31 ± 4	1.5 ± 0.2
0–3	14.6 ± 1.2	9.9 ± 1.5	1.5 ± 0.3
0–4	4.0 ± 0.3	2.9 ± 0.4	1.5 ± 0.3
0–5	1.1 ± 0.2		
1–2	38 ± 8	29 ± 6	1.3 ± 0.4
1–3	26 ± 2	24 ± 4	1.1 ± 0.2
1–4	18 ± 2	13 ± 2	1.4 ± 0.3
1–6	1.54 ± 0.14	2.0 ± 0.7	0.8 ± 0.3
1–7		0.37 ± 0.07	
2–4	8.4 ± 1.6	5.1 ± 0.9	1.6 ± 0.4
2–6		3.1 ± 0.7	
2–7		0.81 ± 0.13	
2–8	0.40 ± 0.08	0.35 ± 0.11	1.1 ± 0.4
3–3	5.6 ± 1.2	5.1 ± 0.7	1.1 ± 0.4
3–4	1.0 ± 0.3	1.1 ± 0.3	0.9 ± 0.4
3–5	2.0 ± 0.6	1.3 ± 0.4	1.5 ± 0.6
3–7		1.1 ± 0.4	
3–8	0.68 ± 0.12	0.52 ± 0.17	1.3 ± 0.5

^a The fluorescent efficiencies are based on measurements in N_2 and air extrapolated to low pressure where collisional deactivation is an insignificant depopulating process. The probable error does not include the error in the absolute measurement which is estimated to be an additional ±15%.

Table 7

Maximum apparent cross-sections of the first four vibration states of the $N_2^+ B^2\Sigma_u^+$ electronic state as given in Ref. [12]

ν	$Q'(\nu)$ (10^{-18} cm ²)
0	22.3
1	2.6
2	0.21
3	0.09

These apparent cross-sections $Q'(\nu)$ are defined as the sum of all optical cross-sections of all bands which have the same upper vibrational state ν' . For low pressures and beam currents, where the optical cross-sections are independent of these variables, $Q'(\nu) = \sum_{\nu''} Q(\nu', \nu'')$. $Q'(\nu)$ also is equal to the true cross-section $Q(\nu')$ of the excitation of ν' plus the sum of the optical cross-sections of all bands cascading to ν' from higher energy states. The excitation functions were measured for the first negative system of N_2^+ up to energies of 450 eV and the functions show broad maxima at about 120 eV for the (0,0) and (1,0) bands. Frank–Condon factors indicated that the measured optical cross-sections account for over 99% of $Q'(0)$ and $Q'(1)$. The maximum apparent cross-sections are given in Table 7.

8.2. Dotchin et al. (1973)

In 1973, Dotchin et al. [13] presented radiative lifetime measurements using a pulsed-proton beam and target gas pressures between 1 and 200 mTorr. They studied two gases, nitrogen and carbon monoxide. For the first negative system of N_2^+ , the measurements were performed at the 3914 Å (0,0) and the

4278 Å (0,1) bands. The mean zero-pressure intercept yielded (60.4 ± 0.4) ns. The lifetimes for the second positive system of nitrogen states were investigated using the 3805 Å (0,2), 4059 Å (0,3), 3755 Å (1,3), 3998 Å (1,4), and the 3711 Å (2,4) transitions. The mean lifetime for $\nu' = 0$ was determined to be (40.4 ± 0.5) ns, for $\nu' = 1$ to (40.6 ± 0.5) ns, and for $\nu' = 2$ to (38.5 ± 0.6) ns.

8.3. Lillicrap (1973)

In the same year, a NASA report about the temperature dependence of collisional quenching was presented [14]. Lillicrap investigated the 391.4 nm line of nitrogen and the 501.6 nm line of helium. The work was performed because of interest in hypersonic flight at high altitudes and here the high-speed, low-density flows were to be studied. The quenching behavior of nitrogen was measured in the temperature interval from 78 to 300 K. In their analysis, only collisions between excited molecules and ground-state molecules of the same species were assumed. The gas was excited by a 30 keV electron beam of 200 μ A. The cooling was realized by a heat exchanger filled with 2-methylbutane for the temperatures between 300 and 113 K and with liquid nitrogen to obtain temperatures close to 78 K. For analyzing the quenching cross-sections, the densities were limited between 1×10^{22} and 12×10^{22} molecules/m³, because of not conceived effects at lower densities. The given uncertainties are only those of individual measurements and no reliable standard deviations. The measured cross-sections are given in Table 8.

8.4. Lofthus and Krupenie (1977)

For a really comprehensive review about “The Spectrum of Molecular Nitrogen”, the reader is referred to Lofthus and Krupenie [15]. Within this review and compilation, data are presented of the observed and predicted spectroscopic data on the molecule N_2 and its ions N_2^+ , N_2^{2+} , and the molecule N_3 . Amongst others, radiative lifetimes and Franck–Condon integrals are given. For example the radiative lifetimes as weighted averages of many experiments are given for the second positive 0–0 transition with $(3.66 \pm 0.05) \times 10^{-8}$ s and for the first negative 0–0 band with $(6.25 \pm 0.08) \times 10^{-8}$ s.

8.5. Itikawa (1986)

In 1986, Itikawa et al. [16] published again a compilation of data about nitrogen with strong emphasis on cross-sections for collisions of electrons and photons. For electron collisions, the processes of total scattering, elastic scattering, momentum transfer, excitations of rotational, vibrational and electronic states, dissociation, and ionization are considered and presented graphically. Spectroscopic and other properties of the nitrogen molecule

Table 8

Cross-sections for quenching of the $\nu' = 0$ level of the $N_2^+ B^2\Sigma_u^+$ state of N_2 as given in Ref. [14]

T (K)	σ_{NN} (m ²)
296	$4.8 \pm 0.2 \times 10^{-19}$
247	$5.6 \pm 0.3 \times 10^{-19}$
208	$6.7 \pm 0.3 \times 10^{-19}$
168	$7.7 \pm 0.2 \times 10^{-19}$
162	$8.7 \pm 0.6 \times 10^{-19}$
123	$9.8 \pm 0.7 \times 10^{-19}$
118	$10.0 \pm 0.8 \times 10^{-19}$
78	$11.0 \pm 0.9 \times 10^{-19}$

Table 9Lifetimes (in units of 10^{-8} s) of electronic states of N_2 and N_2^+ as given in Ref. [16]

v'	$C^3\Pi_u \rightarrow B^3\Pi_g$	$B^2\Sigma_u^+ \rightarrow X^2\Sigma_g^+$
0	3.67	5.52
1	3.65	5.38
2	3.69	5.30
3	3.77	5.27
4	3.94	5.27
5		5.33

are summarized. Also in the work by Itikawa et al. [16], radiative lifetimes are presented, however, these numbers have been calculated theoretically. In Table 9, the values for the second positive and first negative system of nitrogen are reviewed.

8.6. Gilmore et al. (1992)

A more theoretical analysis was published by Gilmore et al. [17]. In this comprehensive report, calculations on the Franck–Condon factors, r -centroids (with r being the internuclear distance), electronic transition moments, and Einstein coefficients for many nitrogen and oxygen band systems are presented. The Einstein coefficients or radiative transition probabilities can be used for calculating emission spectra produced by electrons incident in air. The Franck–Condon factors are the vibrational overlap integrals and are used for calculating the branching ratios for populating various vibrational levels when an electronic state is excited from the ground state by electron impact [17]. The radiative transition parameters of 38 band systems considered in that report are listed in several tables. Also the radiative lifetimes of 14 N_2 , N_2^+ , and O_2^+ states are calculated and listed as a function of vibration level. Since this comprehensive report comprises 86 pages of tables, no data are reviewed here.

8.7. Fons et al. (1996)

The idea of the apparent excitation cross-sections was seized upon again by Fons et al. [18]. The absolute optical emission cross-sections were measured for the second positive system of nitrogen for many transitions from $v' = 0, 1, 2, 3, 4$ and v' up to 9. The electron beam energy was modulated from threshold up to 600 eV and the gas pressure was fixed at about 4 mTorr. The estimated uncertainty for each cross-section is also given in Ref. [18]. For the (0,0) band it is 13%, but for many other bands, the uncertainty is roughly 20%. The apparent electron excitation cross-section of the $C^3\Pi_u(v')$ vibrational level is given as the sum of the optical emission cross-sections of the (v', v'') bands over v'' , because the $C \rightarrow B$ transition is the only radiative decay channel of the $C^3\Pi_u$ state. The absolute and relative values are reviewed in Table 10 and compared with relative Franck–Condon factors calculated by Gilmore et al. [17]. The comparison between the relative $Q_{app}(Cv')$ values and the relative Franck–Condon factors give rise to the discussion about the validity of the Franck–Condon approximation. If the cascade from higher levels is assumed to be small in comparison with the direct excitation cross-section, the apparent excitation cross-section can be compared with the appropriate Franck–Condon factors. For $v' = 0, 1, 2$ the numbers agree rather well, but for $v' = 2-3$ an abrupt decrease both in the relative Franck–Condon factor (or the direct excitation cross-section) and in the relative apparent cross-section can be seen. The authors of Ref. [18] estimated the contribution from the missing optical emission cross-section to the apparent cross-sections to be no more than 1% for $v' = 0, 1, 2$, no more than 4.5% for $v' = 3$, and approximately 10% for $v' = 4$. Finally, they

Table 10Apparent excitation cross-sections (in units of 10^{-18} cm²) for the $C^3\Pi_u(v')$ vibrational levels, $Q_{app}(Cv')$, at incident energies corresponding to the peak of the excitation functions as given in Ref. [18]

v'	$Q_{app}(Cv')$	Relative $Q_{app}(Cv')$	Relative FC factors
0	21.7	1.00	1.00
1	15.2	0.70	0.57
2	5.57	0.26	0.19
3	1.76	0.081	0.055
4	0.88	0.041	0.014

The relative values of these cross-sections in the third column are compared to the relative Franck–Condon (FC) factors.

Table 11Radiative lifetimes τ_0 (in 10^{-9} s) and rate constants k_q^M of deactivation by molecule M (in 10^{-10} cm³ s⁻¹) for $N_2(C^3\Pi_u, v = 0 \dots 4)$ as given in Ref. [19] (2000)

v	τ_0	$k_q^{N_2}$	$k_q^{O_2}$	$k_q^{H_2O}$
0	42 ± 2	0.13 ± 0.02	3.0 ± 0.3	3.9 ± 0.4
1	41 ± 3	0.29 ± 0.03	3.1 ± 0.3	3.7 ± 0.4
2	39 ± 4	0.46 ± 0.06	3.7 ± 0.5	4.0 ± 0.6
3	41 ± 5	0.43 ± 0.06	4.3 ± 0.6	4.5 ± 0.7

concluded that the deviation of the apparent excitation cross-sections from the Franck–Condon relation is consistent with the cascade description and that it does not necessarily signify a breakdown of the Franck–Condon picture [18].

8.8. Pancheshnyi et al. (1997–2000)

Between 1997 and 2000 Pancheshnyi et al. published four reports about rate constants and lifetimes of nitrogen [19]. Here, only the latest one (2000) is reviewed since former data are updated therein. The measurements were performed using emission spectroscopy with sub-nanosecond temporal resolution. The spectral range of the optical system was between 250 and 600 nm. Gas pressures ranged from 0.05 to 30 Torr at a temperature of 295 ± 5 K. The gas was either pure nitrogen or nitrogen mixtures with oxygen, hydrogen or oxygen and hydrogen. It was measured that the excitation occurs up to 25 ns at 1 Torr pressure after discharge and up to 5–6 ns at high pressures. The values of the radiative lifetimes τ were obtained by extrapolation to zero pressure and the quenching rates were determined from the slope of the straight line $1/\tau$ vs. pressure [19] (2000). The uncertainties of the given values are given with 5–15% on average. In Table 11, the radiative lifetimes and the deactivation rate constants are summarized.

9. Fluorescence yield measurements between 1970 and 1996

During mainly the same period as covered in Section 8, only three well-known measurements on nitrogen fluorescence yield were performed.

9.1. Hirsh et al. (1970)

The first publication was by Hirsh et al. [20]. The absolute fluorescence efficiency of the first negative (0,0) transition of N_2^+ was measured in nitrogen and in an air-like $N_2:O_2$ mixture. The incident electron beam covered an energy range from 0.65 to 1.6 MeV, which

Table 12
Fluorescence efficiencies as given in Ref. [21]

Wavelength (Å)	Transition	Efficiencies (%)	
		Nitrogen	Air
3914	N ₂ ⁺ 1st neg. (0,0)	0.66	0.53
3371	N ₂ 2nd pos. (0,0)	0.26	0.21
3805	N ₂ 2nd pos. (0,2)	0.062	0.048
4060	N ₂ 2nd pos. (0,3)	0.018	0.014

had not been studied before then. Under the experimental conditions described in Ref. [20], the incident primary and all resulting secondary electrons ionize the ground-state N₂ molecule. Approximately one 391.4 nm photon is produced for every 15 electron–ion pairs. For the primary electron it was a thin target condition, but for the slow secondary electrons it was a thick target. Ten percent of the ionized molecules are formed in the B²Σ_u⁺ (v' = 0) state which de-excites by the emission of 391.4 nm photons. The resultant fluorescence efficiency,¹⁰ defined as the power radiated by the gas in 391.4 nm photons per unit power deposited in the gas by the electron beam, was determined to $(4.75 \pm 1.5) \times 10^{-3}$ in air and to $(6.0 \pm 1.59) \times 10^{-3}$ in nitrogen. A scan in energy indicated that the fluorescence efficiency is energy-independent from near threshold energy to 1.65 MeV. A pressure scan followed by an extrapolation to zero pressure yielded a reciprocal lifetime of $(1.52 \pm 0.08) \times 10^7$ s⁻¹ for the B²Σ state. The cross-sections for quenching were found to be $(65 \pm 4) \times 10^{-16}$ cm² for nitrogen–nitrogen collisions and $(109 \pm 45) \times 10^{-16}$ cm² for nitrogen–oxygen collisions.

9.2. Mitchell (1970)

In the same year, Mitchell published fluorescence efficiencies and collisional deactivation rates for the second positive bands of N₂ and the first negative band of N₂⁺ [21]. He used soft monochromatic X-rays from the energy range between 0.9 and 8.0 keV. All measurements were performed either in pure nitrogen or in an air-like mixture of 20% O₂ and 80% N₂ at pressures ranging from 0.30 to 600 Torr. Describing the data by the Stern–Volmer relationship

$$1/\eta = (1/\eta_0)(1 + KP), \quad (14)$$

where P is the pressure in Torr and K is the quenching constant in Torr⁻¹, the fluorescence efficiencies¹⁰ were found as given in Table 12. A variation of energy in the given range confirmed that the efficiencies are independent of the X-ray energy. From theory it was known that the deactivation rates should be the same for all bands with the same upper vibrational state. Mitchell could show experimentally that the K values for the second positive v' = 0 bands are the same. Thus he derived a rate constant for the first negative (v' = 0) system for nitrogen–nitrogen quenching of 4.53×10^{-10} cm³/s and for nitrogen–oxygen quenching of 7.36×10^{-10} cm³/s. For the second positive (v' = 0) system, Mitchell obtained for nitrogen–nitrogen quenching a rate constant of 1.12×10^{-10} cm³/s and for nitrogen–oxygen quenching of 3.12×10^{-10} cm³/s [21]. These numbers were calculated applying the lifetime $\tau_0 = 6.58 \times 10^{-8}$ s from Bennett and Dalby [5].

9.3. Kakimoto et al. (1996)

Finally in 1996, the aspects of nitrogen fluorescence emission were again discussed in the context of extensive air shower

¹⁰ In the nomenclature of the summary article [1], this parameter corresponds to Φ_0^0 .

Table 13
Constants A_1 , A_2 , B_1 and B_2 used in Eq. (15) as given in Ref. [22]

A_1	89.0 ± 1.7 m ² kg ⁻¹
A_2	55.0 ± 2.2 m ² kg ⁻¹
B_1	1.85 ± 0.04 m ³ kg ⁻¹ K ^{-1/2}
B_2	6.50 ± 0.33 m ³ kg ⁻¹ K ^{-1/2}

detection by fluorescence telescopes. Kakimoto et al. studied the fluorescence yield¹¹ with electron energies between 1.4 and 1000 MeV [22]. The altitude dependence in the Earth's atmosphere was parameterized and the proportionality between yield and energy deposit of incident particles was checked. The experiment was split into two parts. The first part comprised a 1 mCi⁹⁰Sr source which provided 1.4 MeV electrons for exciting either N₂ gas or dry air. In the second part, the exciting electrons were extracted from a synchrotron with energies of 300, 650, and 1000 MeV. The authors plotted the fluorescence yield vs. electron energy into one plot together with the Bethe–Bloch curve for energy deposit by electrons. The absolute scale was adjusted at 1.4 MeV. The agreement between the curve and the data points is fair, thus Kakimoto et al. concluded the proportionality between fluorescence yield and energy deposit. The fluorescence efficiency¹² for 1.4 MeV electrons at 600 mm Hg in air was measured at three wavelengths. Defined as the radiated energy divided by the energy loss in the observed medium, the efficiency was given at 337 nm as 2.1×10^{-5} , at 357 nm as 2.2×10^{-5} , and at 391 nm as 0.84×10^{-5} [22]. For applying their experimental results to extensive air shower reconstruction, Kakimoto et al. parameterized the fluorescence yield in dependence of energy and altitude as

$$\text{yield} = \frac{(dE/dX)}{(dE/dX)_{1.4 \text{ MeV}}} \rho \left\{ \frac{A_1}{1 + \rho B_1 \sqrt{T}} + \frac{A_2}{1 + \rho B_2 \sqrt{T}} \right\} \quad (15)$$

where dE/dX is the electron energy loss, density ρ in kg/m³, temperature T in Kelvin, and $(dE/dX)_{1.4 \text{ MeV}}$ is the dE/dX evaluated at 1.4 MeV. The experimentally derived constants are reviewed in Table 13.

Acknowledgments

The authors acknowledge the support of the Spanish Ministry of Science and Education MEC (FPA2006-12184-C02-01), Comunidad de Madrid (Ref.: 910600) and CONSOLIDER program, and of the German Research Foundation (DFG) (KE 1151/1-1 and KE 1151/1-2). Further support has been granted by the Radboud Universiteit Nijmegen as well as by the Universität Karlsruhe (TH) and the Forschungszentrum Karlsruhe GmbH which are currently merging their activities in the Karlsruhe Institute of Technology (KIT). The authors would like to thank C. Escobar, C. Field, M. Fraga, K. Martens, M. Nagano, J. Ridky, J. Rosado, and A. Ulrich for valuable comments on the manuscript.

References

- [1] F. Arqueros, J.R. Hörandel, B. Keilhauer, Proceedings of the 5th Fluorescence Workshop, Nucl. Instr. and Meth. A 597 (2008) 1.
- [2] A.E. Grün, E. Schopper, Z. Naturforschg. 9a (1954) 55.
- [3] A.E. Grün, Can. J. Phys. 36 (1958) 858.
- [4] B. Brocklehurst, Trans. Faraday Soc. 60 (1964) 2151.

¹¹ In the nomenclature of the summary article [1], this parameter corresponds to ϵ_{λ} .

¹² In the nomenclature of the summary article [1], this parameter corresponds to Φ_{λ} .

- [5] R.G. Bennett, F.W. Dalby, *J. Chem. Phys.* 31 (1959) 434.
- [6] G. Davidson, R. O'Neil, *J. Chem. Phys.* 41 (1964) 3946.
- [7] L. Wallace, *Astrophys. J. Suppl.* 6 (1962) 445.
- [8] R. O'Neil, G. Davidson, American Science and Engineering, Inc., Report AFCRL-67-0277, Cambridge, MA, 1968.
- [9] A. Bunner, The atmosphere as a cosmic ray scintillator, Thesis, Cornell University, 1964.
- [10] A.N. Bunner, Cosmic ray detection by atmospheric fluorescence, Ph.D. Thesis, Cornell University, 1967.
- [11] P. Hartman, Luminescence efficiency of air on electron bombardment, Los Alamos Report, 1963.
- [12] P.N. Stanton, R.M.S. John, *J. Opt. Soc. Am.* 59 (1969) 252.
- [13] L.W. Dotchin, et al., *J. Chem. Phys.* 59 (1973) 3960.
- [14] D.C. Lillicrap, Collision quenching effects in nitrogen and helium excited by a 30-keV electron beam, NASA-TM-X-2842, 1973.
- [15] A. Lofthus, P.H. Krupenie, *J. Phys. Chem. Ref. Data* 6 (1977) 113.
- [16] Y. Itikawa, et al., *J. Phys. Chem. Ref. Data* 15 (1986) 985.
- [17] F.R. Gilmore, et al., *J. Chem. Ref. Data* 21 (1992) 1005.
- [18] J.T. Fons, et al., *Phys. Rev. A* 53 (1996) 2239.
- [19] S.V. Pancheshnyi, et al., *Plasma Phys. Rep.* 23 (1997) 664;
S.V. Pancheshnyi, et al., *Chem. Phys. Lett.* 294 (1998) 523;
S.V. Pancheshnyi, et al., *J. Phys. D Appl. Phys.* 32 (1999) 2219;
S.V. Pancheshnyi, et al., *Chem. Phys.* 262 (2000) 349.
- [20] M.N. Hirsh, et al., *Phys. Rev. A* 1 (1970) 1615.
- [21] K.B. Mitchell, *J. Chem. Phys.* 53 (1970) 1795.
- [22] F. Kakimoto, et al., *Nucl. Instr. and Meth. A* 372 (1996) 527.